Frequency stabilization of a 214.5-nm ultraviolet laser

Shiguang Wang (王时光)[1,2], Jianwei Zhang (张建伟)[1,3*], Zhengbo Wang (王正博)[1,2], Bo Wang (王 波)[1,3], Weixin Liu (刘维新)[1,3], Yanying Zhao (赵研英)[1,3], and Lijun Wang (王力军)[1,2,3]

[1] *Joint Institute for Measurement Science, Tsinghua University, Beijing 100084, China*

[2] *Department of Physics, Tsinghua University, Beijing 100084, China*

[3] *Department of Precision Instruments and Mechanology, Tsinghua University, Beijing 100084, China*

[*] *Corresponding author: zhangjw@tsinghua.edu.cn*

Received August 24, 2012; accepted September 4, 2012; posted online January 30, 2013

An improved method for stabilizing a frequency-quadrupled 214.5-nm tunable diode laser system is reported. Improvements to the method include a homemade logic circuit and the use of a Fabry-Perot optical spectrum analyzer as a transfer cavity. Lasers locked with this method exhibit megahertz-level frequency stability measured with an optical frequency comb referenced to a cesium atomic standard. The laser can be locked for hours to days, depending on experiment requirements. Being relatively inexpensive, stable, and robust, the control method can be applied to stabilizing essentially all lasers of deep ultraviolet wavelengths.

OCIS codes: 140.7240, 140.2020, 120.2230.
doi: 10.3788/COL201311.031401.

Experiments in optical physics often require lasers with frequency stability of megahertz levels. In our cadmium ion (Cd^+) microwave frequency standard experiment, stabilizing the frequency of the cooling laser to megahertz level is a desirable procedure. The 214.5-nm ultraviolet (UV) laser is the fourth harmonic of an amplified external cavity diode laser oscillating at 858 nm. One method for stabilizing the UV laser is by locking it to a cadmium discharge lamp as reported in Refs. [1,2]. With this method, however, UV laser power should be fed into the lamp to generate error signals. This approach is a non-optimal choice because the output power of the UV laser is limited by the low efficiency of frequency quadrupling. In earlier work[3], Blinov *et al.* locked the second harmonic of an 858-nm laser to the Doppler-free saturated absorption spectrum (SAS) of molecular Tellurium (Te_2), and applied an acousto-optic modulator (AOM) to bridge the gap between the resonance lines of Cd^+ and Te_2. The method requires an AOM, which should be operated at about 720 MHz (for $^{113}Cd^+$) in a double-pass setup, and a Te_2 cell, which requires heating to about 500 °C.

We stabilize the 858-nm seed laser rather than its second or fourth harmonic. One of the most common stabilization methods is to lock the laser to atomic or molecular reference lines[4,5]. In our experiment, however, no such suitable atomic line exists for the 858-nm wavelength. In addressing this problem, the transfer cavity technique is often used as an alternative[6−13]. This technique offers a considerably large locking range, and for the Fabry-Perot (F-P) cavity, mirror separation is repeatedly scanned with a piezoelectric transducer (PZT). Beams from target and reference lasers both pass through the F-P cavity, and two transmission peaks can be observed in one free spectral range (FSR). The target laser can then be locked to the reference laser by maintaining constant separation between the two adjacent peaks. Typically, the two transmission peaks are separated by polarization beamsplitters or filters[6−9]; analog-digital and digital-analog converter cards are also needed[9,10].

In our transfer lock experiment, a homemade logic circuit is developed and used to distinguish between reference and target laser signals. The output signal of the spectrum analyzer is determined with only one detector. The frequency locking method is robust, inexpensive, and requires no software programming. The locked laser can work continuously for hours to days without requiring major maintenance.

The F-P cavity in our experiment is an SA200-Series scanning Fabry-Perot interferometer (ThorLabs) with an FSR of 1.5 GHz and a finesse of more than 200 over a wavelength range of 820 to 1 275 nm. Two beams from the reference and target lasers (approximately 1 mW each) are combined with a 50:50 fiber coupler and simultaneously fed into the F-P cavity. If the scanning range is slightly less than one FSR, only two transmission peaks can be observed during one scan.

For an F-P cavity, we have

$$\begin{cases} d + x_{\rm r} = m \times \lambda_{\rm r} \\ d + x_{\rm t} = n \times \lambda_{\rm t} \end{cases}, \tag{1}$$

where d is the original length of the F-P cavity without scanning; m and n are arbitrary integers; $x_{\rm r}$ and $x_{\rm t}$ denote the positions of the reference and target laser resonant peaks, respectively, when the cavity length is modified through the application of scanning voltage to the PZT; $\lambda_{\rm r}$ and $\lambda_{\rm t}$ represent the wavelengths of the reference and target lasers, respectively.

The logic circuit is shown in Fig. 1, and several key waveforms are shown in Fig. 2. As the wavelength of the 858-nm laser is stabilized, the length of the transfer cavity should also be locked to avoid gradual changes with temperature. We use the logic circuit to automatically lock the length $d + x_{\rm r}$ of the F-P cavity, instead of thermally controlling the optical cavity length[7,10]. In previously proposed methods, offset control requires adjustment every few hours or the use of a more sophisticated program to compensate for length drift[11]. Our method is similar

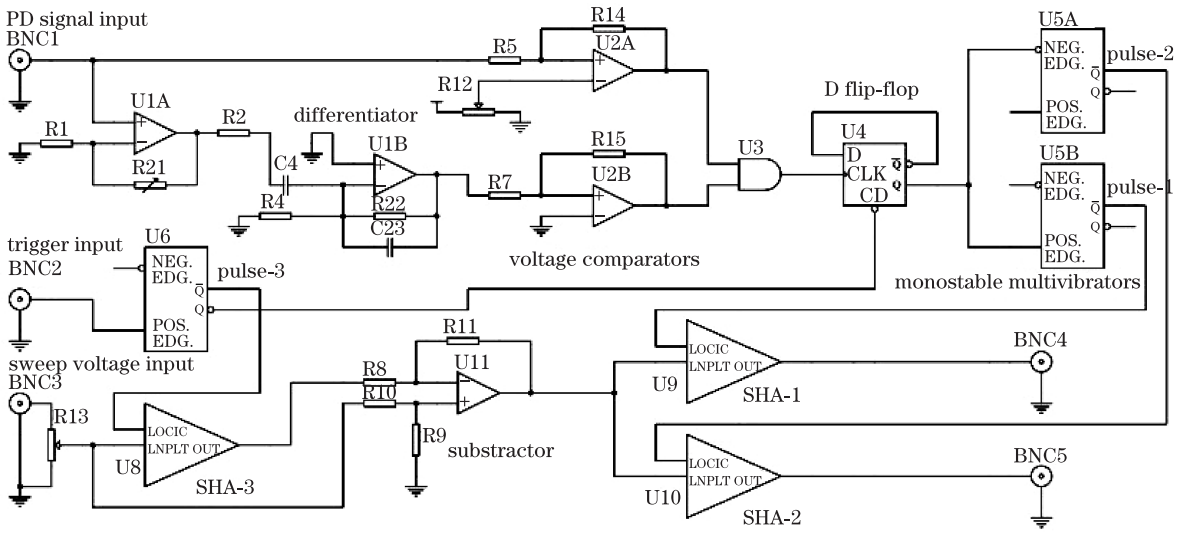

Fig. 1. Schematic of the homemade signal-conditioning circuit. U1 works as a differential amplifier; U2 is a dual-supply voltage comparator; U4 is a dual D-type flip-flop; U5 and U6 are monostable multivibrators; U8, U9, and U10 are sample-and-hold amplifiers. The photodiode signal, trigger signal, and sweep voltage applied to PZT from SA201 are connected to BNC1, BNC2, and BNC3, respectively. The outputs of SHA-1 and SHA-2 are induced by pulse-1 and pulse-2, respectively, and are directed to BNC4 and BNC5.

to a previously reported approach[9], but simplified and does not require temperature control. Locking length difference $x_r - x_t$ also locks the wavelength of the target laser.

The spectrum signal from the F-P cavity (Fig. 2(a)) is pre-amplified and fed into a differential circuit[11] to obtain a dispersive signal that crosses zero at pulse peaks. A hysteresis comparator, U2B, is used to detect the zero-crossing point and eliminate the noise near this zero-crossing voltage. The signal from the hysteresis comparator is gated with another comparator, U2A, whose reference voltage is lower than the smaller of the two peaks. We consequently obtain two positive pulses, whose rising edges are located at the centers of the two spectral peaks (Fig. 2(b)). Next, the two pulses are used to trigger a D flip-flop to produce a digital signal, whose length spans between the rising edges of the two pulses (Fig. 2(c)). This signal is then fed into two monostable multivibrators to separately produce two pulses at the signal's positive (rising) edge and negative (falling) edge; these edges are denoted as pulse-1 and pulse-2, respectively (Fig. 2(e)). The trigger signal (Fig. 2(d)) from the SA201 controller triggers the third monostable multivibrator to produce a pulse at the positive edge of the trigger signal, which is denoted as pulse-3, also shown in Fig. 2(e). The widths of these three pulses are determined by the monostable multivibrator and are approximately 35 μs. First, pulse-3 triggers a sample-and-hold amplifier (SHA-3) to maintain the attenuated sweeping voltage which is applied as an initializing voltage signal to the PZT at the beginning of every sweep. The attenuated sweep voltage is then subtracted by this initial voltage with a subtractor. Then, the resultant signal is fed into two more SHAs (SHA-1 and SHA-2) triggered by pulse-1 and pulse-2, respectively. The output voltages of these SHAs are therefore proportional to the positions of the reference and target lasers during every sweep, relative to the trigger signal. If the peak of the reference laser appears earlier than that of the target laser during one sweep, the output of SHA-1 represents the reference laser and that of SHA-2 represents the target laser, and vice versa. With this mechanism, the pulse sequence becomes irrelevant. The sweep rate in our experiment is 20 Hz.

The output signals from these two SHAs are then fed into two separate analog PID modules to stabilize the length of the cavity and frequency of the 858-nm laser. Changing the locking positions is simply achieved by changing the set points of the PID modules. In

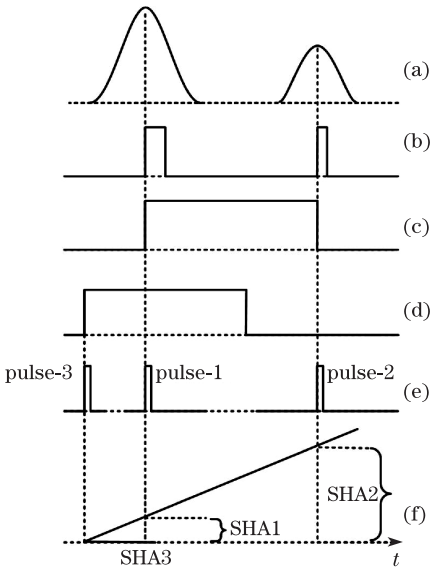

Fig. 2. Schematic signal processing in locking. (a) Spectrum signal from the F-P cavity; (b) signal after the AND gate; (c) signal after the D Flip-Flop; (d) trigger signal from the SA201 controller; (e) three signals from three monostable multivibrators; (f) ramp voltage; SHA-1, SHA-2, and SHA-3 represent the outputs of SHAs triggered by pulse-1, pulse-2, and pulse-3, respectively.

our experiment, we use readily available commercial PID modules (Toptica, PID110). Any simple PID circuit can be used.

To validate the performance of the laser, we measure the frequency stability of the locked 858-nm laser with an optical frequency comb, which is referenced to a cesium atomic clock. For comparison, the free-running laser is also measured with a wavemeter because of its large frequency drift. The results are shown in Fig. 3(a). During the 1-h measurement time, the full-width at half-maximum (FWHM) of the frequency fluctuation of the locked 858-nm laser is 1.2 MHz, a value considerably better than that of the unlocked laser. Given that Allan deviation is commonly used to characterize frequency stability, we also measure and plot the Allan deviation of the locked laser (Fig. 3(b)). The laser has a relative frequency stability of 8×10^{-10} at 1 s and 3×10^{-10} at 500 s.

Three issues should be considered for the laser stabilization method presented in this letter. First, the order of peaks during one sweep is important in distinguishing and separating the peaks of reference and target lasers. Before locking the target laser, the order of the two peaks from the corresponding lasers should be guaranteed correct. Second, the two peaks cannot be too close or cannot overlap; otherwise, the logic locking circuit will not work properly. Fortunately, several lines for cesium can be used to lock a reference laser, thereby avoiding the aforementioned problem. Alternatively, we can change cavity length by adjusting the offset of the F-P cavity controller to separate these peaks. Finally,

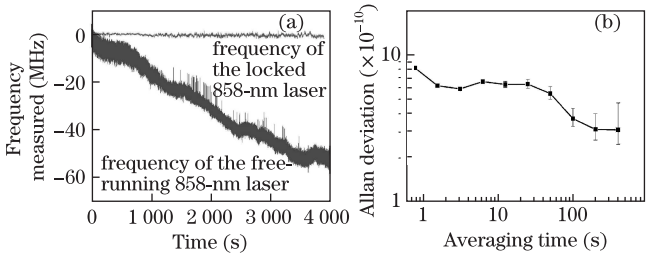

Fig. 3. Measured frequency lock performance. (a) Frequencies of the locked and free-running 858-nm laser measured by the frequency comb and wavemeter, respectively. The frequency shift between these two measurements is subtracted for better illustration. (b) Allan deviation calculated from the result measured with the frequency comb.

with the transfer cavity technique, the frequency of the target laser is locked relative to the reference laser, and its absolute frequency depends on locking parameters. However, this frequency can be easily determined by using a high-resolution wavemeter or from the resonance signal of the discharge in a cadmium lamp[1,2].

In conclusion, we demonstrate an improved, stable, relatively simple, and inexpensive transfer cavity technique for locking a frequency-quadrupled 214.5-nm laser system. Using this method, the frequency of a target laser can be easily locked to megahertz stability while remaining widely tunable. The method can be used to lock lasers that oscillate at any wavelength, especially UV lasers.

This work was supported by the National "973" Program of China (No. 2010CB922901) and the Tsinghua University Scientific Research Initiative Program (No. 20091081474).

References

1. 1. J. I. Kim, C. Y. Park, J. Y. Yeom, E. B. Kim, and T. H. Yoon, Opt. Lett. **28,** 245 (2003).
2. E. W. Streed, T. J. Weinhold, and D. Kielpinski, Appl. Phys. Lett. **93,** 071103 (2008).
3. B. B. Blinov, L. Deslauriers, P. Lee, M. J. Madsen, R. Miller, and C. Monroe, Phys. Rev. A **65,** 040304 (2002).
4. W. Ma, L. Dong, W. Yin, C. Li, and S. Jia, Chin. Opt. Lett. **2,** 486 (2004).
5. Z. Xiong, Y. Long, H. Xiao, X. Zhang, L. He, and B. Lv, Chin. Opt. Lett. **9,** 041406 (2011).
6. B. G. Lindsay, K. A. Smith, and F. B. Dunning, Rev. Sci. Instrum. **62,** 1656 (1991).
7. E. Riedle, S. H. Ashworth, J. T. Farrell, Jr., and D. J. Nesbitt, Rev. Sci. Instrum. **65,** 42 (1994).
8. D. F. Plusquellic, O. Votava, and D. J. Nesbitt, Appl. Opt. **35,** 1464 (1996).
9. W. Z. Zhao, J. E. Simsarian, L. A. Orozco, and G. D. Sprouse, Rev. Sci. Instrum. **69,** 3737 (1998).
10. A. Rossi and V. Biancalana, B. Mai, and L. Tomassetti, Rev. Sci. Instrum. **73,** 2544 (2002).
11. J. H. T. Burke, O. Garcia, K. J. Hughes, B. Livedalen, and C. A. Sackett, Rev. Sci. Instrum. **76,** 116105 (2005).
12. P. Bohlouli-Zanjani, K. Afrousheh, and J. D. D. Martin, Rev. Sci. Instrum. **77,** 093105 (2006).
13. S. M. Jaffe, M. Rochon, and W. M. Yen, Rev. Sci. Instrum. **64,** 2475 (1993).